

## Self-Consistent Energy Bands of Calcium by the Green's-Function Method\*

J. A. DRESEN AND L. PYENSON  
*University of Wyoming, Laramie, Wyoming 82070*  
 (Received 6 July 1970)

The nonrelativistic Green's-function method is used to compute self-consistent energy bands of calcium. The results show the state  $U$  to be occupied in the metal and the state  $W$  to be unoccupied. Corrections due to relativistic effects and to unfreezing of the core are discussed.

### I. INTRODUCTION

There exists in the literature some disagreement concerning the electron-energy-band structure of calcium. An early band-structure calculation for calcium was carried out by Manning and Krutter<sup>1</sup> using the cellular method. They found unoccupied states in the first zone near what would now be called the point  $W$ , and occupied states in the second zone, presumably near  $L$ . A more recent calculation for calcium has been made by Harrison<sup>2</sup> using a few weak constant orthogonalized-plane-wave (OPW) matrix elements. He found a band structure very like that for free electrons, with a Fermi surface consisting of a first-zone monster and second-zone caps at  $L$ .

Altmann and Cracknell<sup>3</sup> have used the modified cellular method of Altmann<sup>4</sup> to calculate the energy bands. They find a band structure that is much less free-electron-like than is the model proposed by Harrison. They find a Fermi surface that consists of small kidney-shaped pockets of holes centered at  $K$  and  $U$  in the zone and a saucer-shaped region of electrons at  $L$ .

The band structure of calcium has been calculated also by Vasvari, Animalu, and Heine,<sup>5</sup> using the model potential of Abarenkov and Heine.<sup>6</sup> Depending upon the choice of the Fermi level, they find<sup>7,8</sup> a first-zone hole surface differing from that given by Harrison and from that given by Altmann and Cracknell, and consisting of hole pockets centered at  $W$ .

Ordinarily, these differences could be resolved by appeal to experimental measurements of the Fermi surface, in particular, to measurements of the de Haas-van Alphen effect. Unfortunately, however, in the case of calcium the measurements<sup>9,10</sup> are incomplete and were made on samples that turned out to be microcrystalline aggregates. As a result, the measurements are subject to differing interpretations and it is possible to make from them a more or less reasonable argument in support of each of the various calculations. Thus, we feel that a reasonably careful first-principles calculation will be useful and will help to choose among the various models proposed for the energy-band structure of calcium.

We have carried out a self-consistent energy-band calculation for calcium using the Green's-function method of Korringa<sup>11</sup> and Kohn and Rostoker.<sup>12</sup>

We find the state  $K$  to be occupied in the first zone and the state  $W$  to be unoccupied, the first-zone Fermi surface consisting of pocket of holes about  $W$ . The second-zone surface consists of the usual saucer-shaped region of electrons at  $L$ .

### II. RESULTS

The first Brillouin zone for the fcc calcium lattice is shown in Fig. 1, where the various symmetry points are labeled.<sup>13</sup> The calculations were carried out for values of  $\mathbf{k}$  in  $1/48$  of the zone, corresponding to 2048 equally spaced points in the full zone. The lattice constant for calcium was chosen as 10.5296 a.u. This value is based upon the measurements of Smith, Carlson, and Vest<sup>14</sup> and includes an estimated correction for thermal contraction to 0°K.

The numerical integrations of the radial Schrödinger equation were carried out for a logarithmic mesh given by

$$x = \ln r = x_0 + (N-1)\Delta x,$$

with  $x_0 = -9$  and  $\Delta x = 0.025$ . The inscribed sphere radius corresponded to  $N=413$ , which gives a value slightly smaller than half the nearest-neighbor distance. The integrations were carried out using a modified Milne method, with the starting values generated by a series expansion near the origin.

The calculations were done nonrelativistically and without spin-orbit coupling since it was felt that the extra computer time that would be needed for relativistic calculations was not justified. These corrections are shown to be small in Sec. III. The calculations were carried out self-consistently, using a procedure generally similar to that described by Snow and Waber<sup>15</sup> in their self-consistent calculation for copper. The calculations were carried out until for all occupied states the energy eigenvalues differed by less than 0.002 Ry between the two final steps.

The starting potential was generated from a superposition of the free-atom charge densities.<sup>16</sup> The crystal-core charge density was calculated from the free-atom core with nearest-neighbors overlap and its value frozen for subsequent steps of the calculation (the effect of removing this restriction is discussed in Sec. III). The potential for succeeding steps in the self-consistent procedure was computed from the

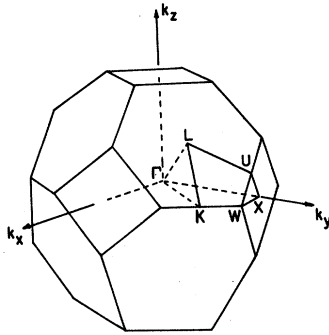


FIG. 1. First Brillouin zone for fcc calcium.

frozen-core density and an average of the conduction electron densities found in the two preceding steps of the calculations. The crystal muffin-tin potential was calculated using the formulation suggested by Liberman,<sup>17</sup> which is particularly suited to this type of calculation. The structure parameters needed for computing the potential from this formulation were found to be

$$\langle 1/r \rangle_R = 1/(0.37832a),$$

$$\langle 1/r_{12} \rangle_{RR} = 1/(0.38157a),$$

where  $a$  is the lattice constant. The values include the correction to apply to the inscribed sphere radius used here and have an estimated uncertainty of about 0.05 and 0.25%, respectively. Liberman's formulation uses the Kohn-Sham<sup>18</sup> exchange potential, which is  $\frac{2}{3}$  as large as that proposed by Slater.<sup>19</sup> Snow and Waber,<sup>15</sup> in their work on copper, found better results by using a value somewhat between these two. We have not investigated the effect of varying this factor for calcium.

As shown by Ham and Segall,<sup>20</sup> it is convenient to expand the wave function used in the Green's-

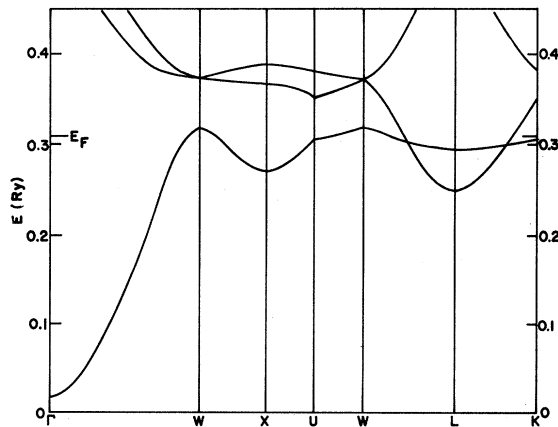


FIG. 2. Self-consistent energy bands for calcium.

TABLE I. Convergence of energy eigenvalues for representative points in the zone. The computed eigenvalues are shown as a function of the maximum  $l$  value included in the trial wave function. The units of  $k$  are  $\pi/4a$  and the energy is given in Ry.

$k$	$l=0$	$l=1$	$l=2$	$l=3$	$l=4$
110	0.02934	0.03029	0.03023	0.03023	0.03023
340	0.18638	0.19833	0.18352	0.18336	0.18336
282	-0.15224	-0.15224	0.30672	0.30593	0.30585
480	-0.15224	-0.15224	0.31887	0.31770	0.31765

function method in the form

$$\psi = \sum_{l,m} i^l d_{lm} R_l(r) Y_{lm}(\theta, \phi),$$

where the  $Y_{lm}$  are real angular functions. This form allows the expansion coefficients to be chosen real and leads to real matrix elements. For these calculations we have included in the expansion all terms through  $l=4$ . The effect on the convergence of the energy eigenvalues of including the higher  $l$  components in the wave function is indicated in Table I. This table gives for some representative points the variation of the computed energy eigenvalue as higher  $l$  values are added to the trial wave function. Particularly noticeable from this table is the large effect produced by the inclusion of the  $l=2$  terms. The importance of these  $d$  terms for calcium has already been stressed by Vasvari, Animalu, and Heine.<sup>5</sup>

Equally important for a self-consistent calculation is the convergence of the wave function itself. An approximate, but convenient, measure of this convergence is afforded by the variation with  $l$  of the fraction of the wave function outside the inscribed sphere. This fraction  $\omega$ , which is needed in the calculations, can conveniently be found by the method given by Ham and Segall.<sup>20</sup> The variation of this fraction with  $l$  is shown for some representative points in Table II, which indicates the degree of convergence obtained for the wave functions used in the calculations.

The final computed energy eigenvalues are given in Table III and the resulting band structure is shown

TABLE II. Convergence of the wave function for representative points in the zone. The table gives the fraction  $\omega$  of the wave function outside the inscribed sphere shown as a function of the maximum  $l$  value included in the trial wave function. The variation of this fraction is assumed to be a measure of convergence. The first column gives  $k$  in units of  $\pi/4a$ .

$k$	$l=0$	$l=1$	$l=2$	$l=3$	$l=4$
110	0.36125	0.33670	0.33645	0.33650	0.33650
340	0.66395	0.37545	0.32760	0.32670	0.32660
282			0.34235	0.33710	0.33645
480			0.34315	0.33575	0.33540

TABLE III. Eigenvalues for points in  $1/48$  of the Brillouin zone considering 2048 points in the entire zone. The units for  $k$  are  $\pi/4a$  and the energy eigenvalues are given in Ry, relative to the constant value  $V_c = -0.3947$  between spheres.

	Band 1	Band 2	Band 3		Band 1	Band 2	Band 3
$k$	$E_1$	$E_2$	$E_3$	$k$	$E_1$	$E_2$	$E_3$
000	0.0173	0.4992	0.5792	221	0.0737	0.4438	0.5040
010	0.0238	0.4918	0.5713	231	0.1033	0.4237	0.4928
020	0.0429	0.4728	0.5501	241	0.1424	0.4029	0.4686
030	0.0737	0.4478	0.5184	251	0.1885	0.3838	0.4396
040	0.1144	0.4220	0.4819	261	0.2367	0.3689	0.4135
050	0.1620	0.3992	0.4467	271	0.2777	0.3615	0.3925
060	0.2114	0.3816	0.4171	281	0.2949	0.3624	0.3810
070	0.2529	0.3706	0.3959				
080	0.2705	0.3669	0.3874	331	0.1316	0.4062	0.4782
				341	0.1691	0.3876	0.4568
110	0.0302	0.4846	0.5693	351	0.2132	0.3698	0.4325
120	0.0492	0.4669	0.5526	361	0.2594	0.3556	0.4106
130	0.0798	0.4436	0.5036	371	0.2974	0.3511	0.3914
140	0.1202	0.4194	0.4763	381	0.3105	0.3600	0.3770
150	0.1675	0.3978	0.4431				
160	0.2167	0.3811	0.4145	441	0.2041	0.3703	0.4399
170	0.2581	0.3706	0.3940	451	0.2447	0.3523	0.4218
180	0.2758	0.3670	0.3858	461	0.2860	0.3378	0.4060
				471	0.3099	0.3431	0.3909
220	0.0677	0.4520	0.4999				
230	0.0976	0.4326	0.4875	551	0.2796	0.3330	0.4108
240	0.1371	0.4123	0.4628	561	0.3051	0.3246	0.4014
250	0.1835	0.3940	0.4330				
260	0.2319	0.3797	0.4068	222	0.0915	0.4259	0.5072
270	0.2728	0.3706	0.3886	232	0.1201	0.4049	0.4979
280	0.2903	0.3675	0.3815	242	0.1582	0.3835	0.4755
				252	0.2031	0.3636	0.4485
330	0.1263	0.4182	0.4688	262	0.2507	0.3482	0.4223
340	0.1642	0.4030	0.4437	272	0.2912	0.3427	0.3973
350	0.2087	0.3892	0.4161	282	0.3058	0.3509	0.3798
360	0.2549	0.3784	0.3930				
370	0.2931	0.3714	0.3796	332	0.1473	0.3833	0.4910
380	0.3084	0.3690	0.3765	342	0.1834	0.3613	0.4745
				352	0.2260	0.3406	0.4521
440	0.1998	0.3933	0.4188	362	0.2718	0.3238	0.4279
450	0.2408	0.3846	0.3926	372	0.3051	0.3246	0.4014
460	0.2818	0.3724	0.3779				
470	0.3104	0.3671	0.3735	442	0.2164	0.3384	0.4647
480	0.3176	0.3721	0.3721	452	0.2550	0.3167	0.4490
				464	0.2948	0.3001	0.4299
550	0.2757	0.3675	0.3810				
560	0.3045	0.3518	0.3784	552	0.2832	0.2982	0.4405
570	0.3105	0.3600	0.3770				
				333	0.1725	0.3585	0.4934
660	0.3058	0.3509	0.3798	343	0.2058	0.3342	0.4831
				353	0.2448	0.3120	0.4646
111	0.0366	0.4772	0.5726	363	0.2832	0.2982	0.4405
121	0.0554	0.4599	0.5572				
131	0.0857	0.4377	0.5023	443	0.2339	0.3091	0.4809
141	0.1258	0.4146	0.4748	453	0.2587	0.2949	0.4689
151	0.1729	0.3939	0.4426				
161	0.2218	0.3777	0.4144	444	0.2457	0.2934	0.4863
171	0.2633	0.3682	0.3936				
181	0.2810	0.3662	0.3844				

in Fig. 2. By assigning an appropriate weight<sup>15</sup> to each of the states given in the table, we find for the Fermi energy, relative to the bottom of the band, the value

$$E_F = 0.3091 - 0.0173 \\ = 0.2918 \text{ Ry.}$$

This value is indicated in Fig. 2. It is particularly to be noted from the table and the figure that we find the point  $W$  to lie above the Fermi level and the point  $U$  to lie below. This is in contrast to the findings of Altmann and Cracknell,<sup>8</sup> but agrees with the conclusions reached by Vasvari.<sup>8</sup> The resulting Fermi surface is very similar to that given and discussed by Vasvari.

### III. ENERGY CORRECTIONS

In this section we discuss two of the corrections—not necessarily the largest—that apply to the calculations discussed above. These corrections involve relativistic effects, including particularly spin-orbit coupling, and the effect of unfreezing the crystal-core charge density. Both corrections are expected to be small for calcium.

Although the calculations discussed in the preceding section were carried out using the nonrelativistic version of the Green's-function method, we have also written programs that are being used for other calculations which use a relativistic version<sup>21,22</sup> of the method. Thus, it was comparatively easy to investigate relativistic corrections to the computed energy eigenvalues. We have used the final crystal muffin-tin potential generated in the nonrelativistic calculations to recompute the energy eigenvalues for a few representative points with the relativistic version of the program. The results of these calculations are shown in Table IV. It is seen from this table that the relativistic corrections are indeed small for calcium and have the effect of further depressing  $U$  relative to  $W$ .

It is customary in self-consistent energy-band calculations to consider only the variation of the conduction-electron charge density, with the core being frozen at the free-atom value. However, changes

in the outer-electron charge density will, of course, react back on the core and this in turn will affect the potential seen by the conduction electrons. To investigate the size of this effect in calcium, we have computed the change in the energy eigenvalues which is produced by unfreezing the core. For this purpose we have first recalculated the free-atom charge density, using a method similar to that described by Liberman, Waber, and Cromer.<sup>16</sup> This preliminary step was necessary to ensure that possible differences in details of methods of calculation would not mask the effect being investigated. The core charge density was then recalculated using the same program, but with the outer  $4S\frac{1}{2}$  conduction-electron charge density frozen at the final value computed in the previous section. The difference between the recalculated free-atom core density and the core density as computed with the frozen  $4S\frac{1}{2}$  electron density was taken to be the correction that is to be added to the crystal-core density used for the calculations described in the preceding section. A new crystal muffin-tin potential was then calculated from this new core density and the final conduction-electron density, as described in Sec. II. The change in the energy eigenvalues that resulted from using this new potential are shown<sup>23</sup> for some representative points in Table IV. It is seen from this table that the correction is reasonably small. This is, of course, not surprising, since the conduction electrons in calcium account for only 10% of the total charge density and, as indicated in Table III, 30% of this is outside the core region. Thus, changes in the conduction-electron charge density from the free-atom value should have a rather small effect on the core. The corrections, however, could be considerably larger for cases, such as copper, where the band electrons account for a proportionately larger fraction of the total charge.

*Note added in proof.* A calculation of the energy-band structure of calcium by the OPW method has recently been reported by Chatterjee and Chakraborti [S. Chatterjee and D. K. Chakraborti, J. Phys. C **3**, S120 (1970)]. These authors find the state  $W$  to be occupied in calcium and the state  $K$  to be unoccupied. This agrees with the conclusions of Altmann and Cracknell,<sup>8</sup> but disagrees with the calculations of Vasvari, Animalu, and Heine<sup>5</sup> and with the calculations reported here.

### ACKNOWLEDGMENTS

We wish to thank Dr. D. A. Liberman of the Los Alamos Scientific Laboratory for making available to us his free-atom results, which were used to generate the starting potential and to construct the core density used in most of the calculations. We wish to thank also the staff of the computer center of the University of Wyoming, without whose cooperation the calculations could not have been made.

TABLE IV. Energy corrections for representative points in the zone. The first column gives  $k$  in units of  $\pi/4a$  and the second column gives the uncorrected energy eigenvalue in Ry. The third and fourth columns give the energy corrections due to relativistic effects and to unfreezing of the core, respectively.

$k$	$E$	$\Delta E$ (rel.)	$\Delta E$ (core)
110	0.03023	-0.00472	-0.00272
340	0.18336	-0.00399	-0.00338
282	0.30585	-0.00116	-0.00534
480	0.31765	-0.00088	-0.00564

\* Submitted by one of the authors (L.P.) in partial fulfillment of the requirements for the M.S. degree from the University of Wyoming.

- <sup>1</sup> M. F. Manning and H. M. Krutter, Phys. Rev. **51**, 761 (1937).
- <sup>2</sup> W. A. Harrison, Phys. Rev. **131**, 2433 (1963).
- <sup>3</sup> S. L. Altmann and A. P. Cracknell, Proc. Phys. Soc. (London) **84**, 761 (1964).
- <sup>4</sup> S. L. Altmann, Proc. Roy. Soc. (London) **A244**, 141 (1958).
- <sup>5</sup> B. Vasvari, A. O. E. Animalu, and V. Heine, Phys. Rev. **154**, 535 (1967).
- <sup>6</sup> I. Abarenkov and V. Heine, Phil. Mag. **12**, 529 (1965).
- <sup>7</sup> B. Vasvari and V. Heine, Phil. Mag. **15**, 731 (1967).
- <sup>8</sup> B. Vasvari, Rev. Mod. Phys. **40**, 776 (1968).
- <sup>9</sup> T. Berlincourt, in *Proceedings of the Seventh International Conference on Low-Temperature Physics* (University of Toronto Press, Toronto, 1960), p. 231.
- <sup>10</sup> J. H. Condon and J. A. Marcus, Phys. Rev. **134**, A446 (1964).
- <sup>11</sup> J. Korrington, Physica **13**, 392 (1947).

- <sup>12</sup> W. Kohn and N. Rostoker, Phys. Rev. **94**, 1111 (1954).
- <sup>13</sup> L. P. Bouchaert, R. Smoluchowski, and E. Wigner, Phys. Rev. **50**, 58 (1936).
- <sup>14</sup> J. F. Smith, O. N. Carlson, and R. W. Vest, J. Electrochem. Soc. **103**, 409 (1956).
- <sup>15</sup> E. C. Snow and J. T. Waber, Phys. Rev. **157**, 570 (1967).
- <sup>16</sup> D. Liberman, J. T. Waber, and D. T. Cromer, Phys. Rev. **137**, A27 (1965).
- <sup>17</sup> D. Liberman, Phys. Rev. **153**, 704 (1967).
- <sup>18</sup> W. Kohn and L. J. Sham, Phys. Rev. **140**, A1133 (1965).
- <sup>19</sup> J. C. Slater, Phys. Rev. **81**, 385 (1951).
- <sup>20</sup> F. S. Ham and B. Segall, Phys. Rev. **124**, 1786 (1961).
- <sup>21</sup> Y. Onodera and M. Okazaki, J. Phys. Soc. Japan **21**, 1273 (1966).
- <sup>22</sup> S. Takada, Prog. Theoret. Phys. (Kyoto) **36**, 224 (1966).
- <sup>23</sup> The magnitude of the entries given in Table IV have been reduced by 0.00068 Ry to account for a change in the constant potential between spheres.

## Interaction of Dislocations with Electrons and with Phonons\*

A. HIKATA, R. A. JOHNSON, AND C. ELBAUM

*Brown University, Providence, Rhode Island 02912*

(Received 8 July 1970)

The interaction parameter of moving dislocations with electrons and with phonons was determined in aluminum, in the temperature range 10 to 250°K. A new technique, involving a "dynamic bias stress", was developed for measuring ultrasonic-attenuation changes  $\Delta\alpha$ . The numerical values of the interaction parameter were obtained from the measured  $\Delta\alpha$  by means of an analysis which does not require any knowledge of the dislocation density or of other inaccurately known features of the dislocation network. The results indicate that the dislocation interaction with electrons is temperature independent and the interaction with phonons increases with increasing temperature. These results are consistent with theoretical predictions.

### I. INTRODUCTION

When a dislocation in a crystal is set in motion, it experiences a resistive force against its motion. In the string model of a vibrating dislocation, this frictional force, or damping, is usually assumed to be proportional to the dislocation velocity and is described formally by the following equation:

$$Bv = b\tau, \quad (1)$$

where  $b\tau$  is the force per unit length acting on a dislocation moving with velocity  $v$ ,  $b$  is Burgers's vector,  $\tau$  is the resolved shear stress on the dislocation slip system, and  $B$  is the damping constant. This damping constant is assumed here to consist of two parts, one due to interactions of dislocations with phonons ( $B_{ph}$ ) and the other due to interactions with conduction electrons ( $B_e$ ). It is further assumed that these parts are additive, i.e.,  $B = B_{ph} + B_e$ .

Theoretical attempts to predict the magnitude and temperature dependence of  $B_{ph}$  have been made in the past by a number of people including Eshelby,<sup>1</sup> Leibfried,<sup>2</sup> Nabarro,<sup>3</sup> Lothe,<sup>4</sup> Weiner,<sup>5</sup> Mason,<sup>6</sup> and Seeger<sup>7</sup>; and for the electron contribution  $B_e$ , by Mason,<sup>8</sup> Kravchenko,<sup>9</sup> Holstein,<sup>10</sup> and Brailsford.<sup>11</sup>

Comparison and discussion of some of these predictions are presented by Nabarro.<sup>12</sup>

Commonly used techniques for experimental determination of the damping constant  $B$  are (i) direct observation by etch pits<sup>13</sup> or x rays<sup>14</sup> of the displacement of individual dislocations produced by stress pulses of known magnitude and duration, (ii) ultrasonic-attenuation methods,<sup>15-18</sup> and (iii) macroscopic mechanical tests.<sup>19-21</sup> Discussions concerning the relation between the values of damping constants deduced by these methods were given by Fanti *et al.*<sup>22</sup> and by Gillis *et al.*<sup>23</sup> The purpose of this paper is to discuss a new method of obtaining the damping constant by means of ultrasonic measurements and to present experimental values deduced from this approach. With this new method we have overcome many difficulties previously encountered both in the analysis and in the experimental technique. The analysis is applied to the case of aluminum and the value of  $B$  thus derived and its temperature dependence are presented.

In Sec. II, the method of analysis is described. The new experimental technique, a dynamic bias stress method, is outlined in Sec. III. The results obtained in aluminum single crystals are given in Sec. IV and